Article

Effect of *Acidithiobacillus ferrooxidans* on Humic-Acid Passivation Layer on Pyrite Surface

Hongying Yang [1,*], Wenjie Luo [1,*] and Ying Gao [2]

[1] School of Metallurgy, Northeastern University, Shenyang 110819, China
[2] College of Chemistry, Chemical Engineering and Environmental Engineering, Liaoning Shihua University, Fushun 113001, China; yychengbao_1983@126.com
[*] Correspondence: yanghy@smm.neu.edu.cn (H.Y.); lwj66463863@126.com (W.L.);
   Tel.: +86-24-8367-3932 (H.Y.); +86-24-8367-3932 (W.L.)

Abstract: The effect of *Acidithiobacillus ferrooxidans* on the humic-acid passivation layer on pyrite surfaces was studied by atomic-force microscopy, leaching experiments, and adsorption experiments. Atomic-force-microscopy results showed that humic-acid was adsorbed onto the pyrite surface. The bacteria grew and reproduced on the humic-acid layer. Leaching experiments showed that the humic-acid passivation layer prevented the oxidation of pyrite by Fe^{3+} under aseptic conditions. Bacteria destroyed the humic-acid layer, promoted pyrite oxidation, and increased the oxidation of pyrite from 1.64% to 67.9%. Bacterial adsorption experiments showed that the humic-acid passivation layer decreased the speed of bacterial adsorption on the pyrite surface but had no effect on the number of bacteria adsorbed on the pyrite surface. The maximum number of bacteria adsorbed by pyrite with and without the humic-acid layer was 4.17×10^{10} cells·mL^{-1} and 4.4×10^{10} cells·mL^{-1}, respectively. Extracellular polymeric stratum layer of bacteria cultured at different concentrations of humic-acid was extracted and analyzed. This layer could destroy the humic-acid layer and promote pyrite oxidation.

Keywords: pyrite; humic-acid; *Acidithiobacillus ferrooxidans*; adsorption; atomic force microscopy

1. Introduction

With the depletion of easily treated gold resources, the exploitation and utilization of refractory gold resources of the Carlin-type has attracted the attention of countries globally. Carlin-type gold deposits have two notable features, namely, that the gold is very fine and is often locked in sulfide minerals, such as pyrite [1,2], and second, that gold deposits are rich in humic-acid and other organic matter [3–5]. Humic-acid is a large-molecule organic substance that contains groups such as carboxyl, phenol, hydroxyl, quinine, and ketone. It has a high physiological activity, and exhibits good absorption, complexation, and exchange properties [6,7].

Bacterial oxidation is the main gold-extraction process for Carlin-type gold deposits [8,9]. In this process, the pyrite oxidation rate is correlated positively with the gold recovery rate. Bacteria adsorbed on the pyrite surface can promote pyrite oxidation [10–12]. Previous studies have shown that humic-acid is readily adsorbed on pyrite surfaces, and forms an effective passivation layer, which prevents pyrite oxidation [13–15]. Sorrenti et al. reported that humic-acid adsorption on pyrite is irreversible and that the humic-acid can't be removed by washing [14]. Jeremy et al. reported that bacteria can adsorb humic-acid [16]. No research exists on the effect of bacteria on the humic-acid passivation layer, which is important in the application of bacterial oxidation in Carlin-type gold deposits.

In this study, the morphology of the humic-acid layer on the pyrite surface after adsorption of humic-acid and bacteria were imaged by atomic force microscopy (AFM). Combined with adsorption, leaching and bacterial extracellular polymeric stratum (EPS) experiments, the effect of bacteria on humic-acid layer on pyrite surface was studied.

2. Materials and Methods

2.1. Pyrite Samples

Pyrite samples were from Hunan, China. X-ray diffraction (XRD, X'Pert Pro diffractometer PANalytical B.V., Almelo, The Netherlands) (Figure 1) indicated that the samples were single-crystal pyrite. The scanning angle range was 89° to 5°. The scanning step size was 0.02° and the scanning interval was 4 s.

Pyrite powder was produced by using a rod mill (XMB-68, Wuhan, Hubei, China) and was stored in a sealed glass bottle. The percentage of particles smaller than 36 μm was 85%.
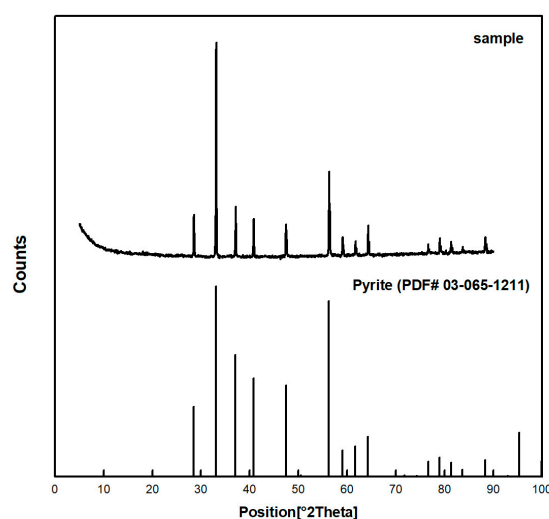

Figure 1. XRD diffraction patterns of pyrite samples.

2.2. Bacteria and Culture Medium

The *Acidithiobacillus ferrooxidans* bacteria were from the biological metallurgy laboratory of the Northeastern University (Shenyang, Liaoning, China). Bacteria were cultured in 9 K medium at pH 1.2 to 1.8.

The 9 K medium consisted of ammonium sulfate (3 g·L^{-1}), potassium hydrogen phosphate (0.5 g·L^{-1}), magnesium sulfate (0.5 g·L^{-1}), calcium nitrate (0.01 g·L^{-1}), and ferrous ions (9 g·L^{-1}). The medium pH was adjusted by using sulfuric acid.

2.3. Adsorption Experiments

Pyrite powder (0.2 g) was added to a humic-acid solution (2 g·L^{-1} and pH 2.0) and left for 4 h. After adsorbing the humic-acid, the pyrite powder was added to the bacterial solution (100 mL) for bacterial adsorption. The amount of adsorbed bacteria was determined by the Ninhydrin method [17].

2.4. Leaching Experiments

Pyrite powder (2 g) was added to a humic-acid solution (0.5 g·L^{-1}) and left for 4 h in a shake flask. After centrifugation, the pyrite with humic-acid was added to either a bacterial solution (redox potential Eh $\geq$ 680 mV) or an aseptic Fe^{3+} solution (9 g·L^{-1}) for the oxidative leaching experiments. The percentage pyrite oxidation was determined by analyzing the total iron concentration in solution.

2.5. Preparation of Atomic-Force Microscopy (AFM) Samples

Pyrite samples were cut into 10 mm × 10 mm × 5 mm blocks and polished with a polishing machine. The treated pyrite blocks were soaked in a 0.5 g·L^{-1} humic-acid solution at pH 1.2 for 1 h. The blocks were removed and rinsed with pH 1.2 water (a mixture of water and sulfuric acid). The samples were dried with natural ventilation and examined by AFM. The pyrite with adsorbed humic-acid was placed in the bacterial culture solution (200 mL) for 0.5, 8, or 16 h, and imaged by AFM after drying under natural ventilation.

AFM imaging of samples was performed using a scanner J that was connected to a MultiMode 8 (Bruker, Karlsruhe, Germany). The topography images were obtained by using tapping mode in air and by using a gold reflex-coated probe (SNL-10 Bruck, Billerica, MA, USA) at a 1 Hz scan rate and 512 lines per sample [18,19]. The AFM measurements were conducted at room temperature (23 $\pm$ 1 °C).

2.6. Extraction and Determination of Bacterial EPS Layer

Bacteria were cultured in 9 K medium that contained different concentrations of humic-acid. When the bacterial concentration reached 10^8 cells·mL^{-1}, the EPS layer of the bacteria was extracted by using the sulfuric-acid method [20]. The extracted EPS solution was dried by vacuum freeze drying method, and the EPS powder was weighed. The humic-acid contents were determined by the modified Lowry method [21].

3. Results and Discussion

3.1. Visual Characteristics of Humic-Acid Layer on Pyrite Surface

AFM was used to image the pyrite surface before and after humic-acid adsorption. Figure 2a,b present three-dimensional (3D) and two-dimensional (2D) images, respectively, of pyrite without humic-acid and show that the pyrite surface was relatively rough with many bulges and low-lying areas. The fractured surface topography was caused by crushing. The pyrite was treated with humic-acid, which, as shown in Figure 2c,d, yielded many bumps on the pyrite surface. Compared with Figure 2a,b, the height of the surface bulges increased significantly, which indicated that large amounts of humic-acid were adsorbed on the pyrite surface and formed a humic-acid layer.
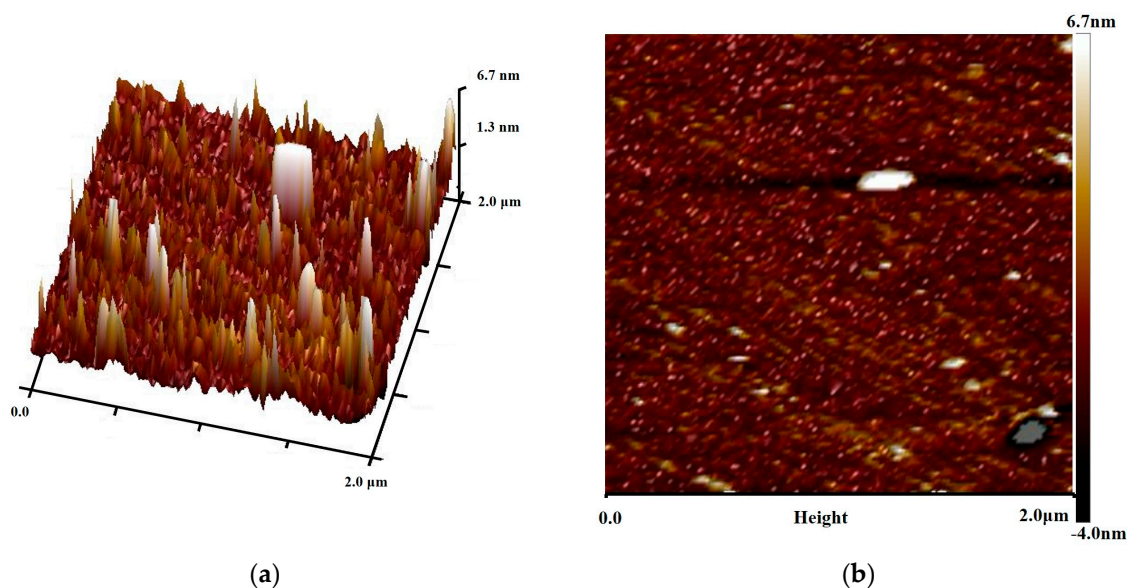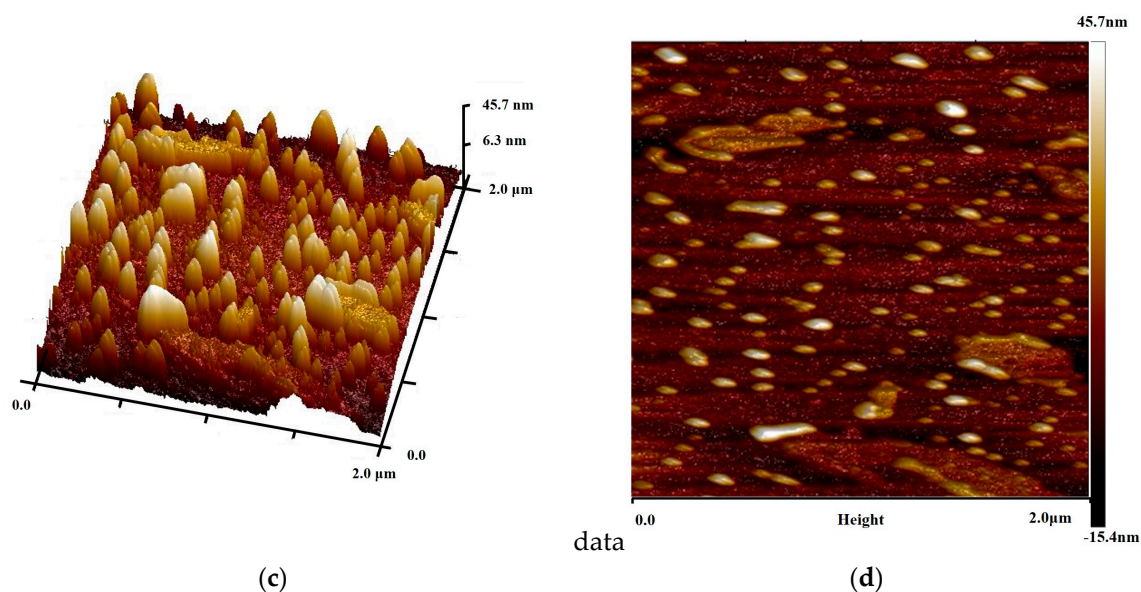

(a)   (b)

Figure 2. *Cont.*

45.7nm

45.7 nm

6.3 nm

2.0 μm

0.0

0.0

2.0 μm

0.0   Height   2.0μm

data

-15.4nm

(**c**)   (**d**)

Figure 2. AFM (**a**) 3D and (**b**) 2D images of pyrite, AFM (**c**) 3D and (**d**) 2D images of pyrite with humic-acid.

3.2. Oxidation of Pyrite with Humic-Acid Layer

Figure 3 shows the percentage oxidation of pyrite with a humic-acid layer under bacterial and aseptic conditions. Under aseptic conditions, Fe^{3+} was used as the oxidant in leaching for 24 days and yielded a 1.61% pyrite-oxidation. The humic-acid layer almost completely inhibited pyrite oxidation. In the presence of bacteria, the pyrite-oxidation percentage increased slowly in the first 4 days, and the corresponding oxidation percentage was 1.82%. The pyrite-oxidation percentage increased significantly after 4 days and reached 67.9% after 24 days.
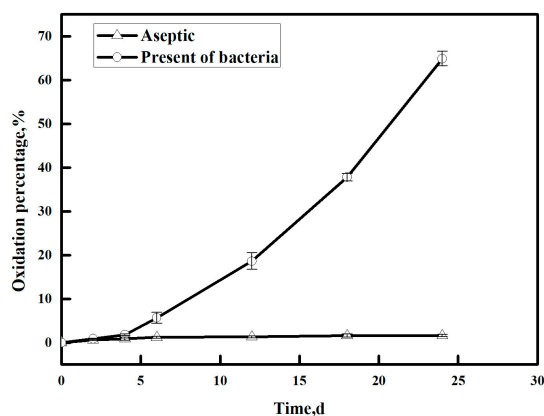

Figure 3. Trend in oxidation of pyrite with humic-acid layer.

Bacteria promote pyrite-oxidation by direct and indirect mechanisms [22,23]. For direct oxidation, it is necessary for the bacteria to contact the pyrite. In indirect oxidation, Fe^{3+} contacts the pyrite for oxidation, Fe^{2+} is oxidized to Fe^{3+} by bacteria, and Fe^{3+} continues to oxidize the pyrite. Humic-acid was adsorbed rapidly on the pyrite surface, which could prevent bacteria and Fe^{3+} contact with pyrite and therefore, pyrite-oxidation was prevented. In the presence of bacteria, the oxidation of pyrite that was passivated by humic-acid was possible and the corresponding oxidation percentage reached 67.9%. Therefore, bacteria promoted pyrite-oxidation by destroying the humic-acid passivation layer.

3.3. Adsorption of Bacteria onto Pyrite

Humic-acid adsorbed on the pyrite surface to change the surface chemical properties. The adsorption of bacteria depends mainly on the electrostatic interactions [23]. Therefore, the humic-acid layer could affect bacterial adsorption on the pyrite surface. Figure 4 shows the number of adsorbed bacteria on the pyrite with or without a humic-acid layer. The adsorbed bacteria without a humic-acid layer reached a saturation value of 4.17×10^{10} cells·g^{-1} in 1 h and remained at 4.14×10^{10} cells·g^{-1} after 2 h. For the pyrite with a humic-acid layer, the number of adsorbed bacteria increased slowly to 0.5×10^{10} cells·g^{-1} during the initial 4 h. The number of adsorbed bacteria increased rapidly at 4–6 h. The number of adsorbed bacteria reached 4.14×10^{10} cells·g^{-1} at 13 h. The adsorbed number remained stable after the maximum adsorption capacity.

The humic-acid layer decreased the bacterial adsorption speed but did not change the amounts of adsorbed bacteria. The humic-acid layer changes the hydrophobicity and pyrite surface charge. The EPS layer on the bacterial surface changes with the environment [24,25]. After initial contact of the EPS with the humic-acid layer, humic-acid stimulates a modification of the EPS layer composition. When the modification of the EPS layer is complete, the bacteria that are adsorbed on the humic-acid layer begin to grow and propagate.
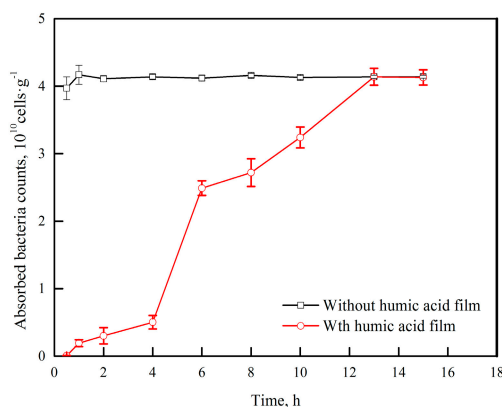

Figure 4. Trend in adsorption of bacteria on pyrite with time.

3.4. Effect of Humic-Acid on Bacterial Surface EPS

The composition of the EPS of the bacteria changes depending on the growth environment. Therefore, the bacterial surface charge and hydrophobicity change, and the bacteria adapt to the environment [26,27]. To study the interactions between the bacteria and humic-acid, bacteria were cultured in 9 K culture medium that contained different concentrations of humic-acid, and the yields of EPS and humic-acid contents of the EPS were determined.

Figure 5 shows that the humic-acid concentration increased, and the EPS production by the bacteria increased significantly. The humic-acid content in the EPS also increased significantly from 0.2% to 7.35%.

Jeremy et al. proposed that humic-acid can be adsorbed by bacteria; it interacts with the bacteria and affects their growth [20]. Our results showed that humic-acid stimulated the secretion of EPS by bacteria, and the EPS layer could adsorb the humic-acid.
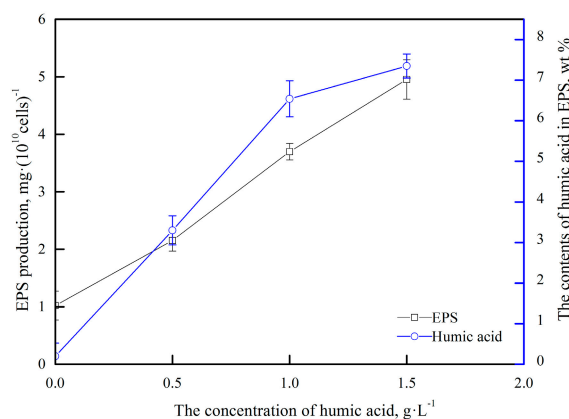
Figure 5. Trend in EPS and humic-acid contents in EPS for different humic-acid concentrations.

3.5. Mechanism of Interaction between Bacteria and Humic-acid Layer

The experimental results in Section 3.1 showed that humic-acid could adsorb rapidly on the pyrite surface. The humic-acid layer could prevent bacterial and Fe^{3+} contact with pyrite, which hindered pyrite oxidation. However, bacteria could promote the oxidation of pyrite.

As shown in Figure 6, the surface of the pyrite with a humic-acid layer, which had been soaked in bacterial solution for 0.5 h, retained bumps with no clear bacterial adsorption on the pyrite surface. Compared with Figure 2d, the surface height changed minimally.
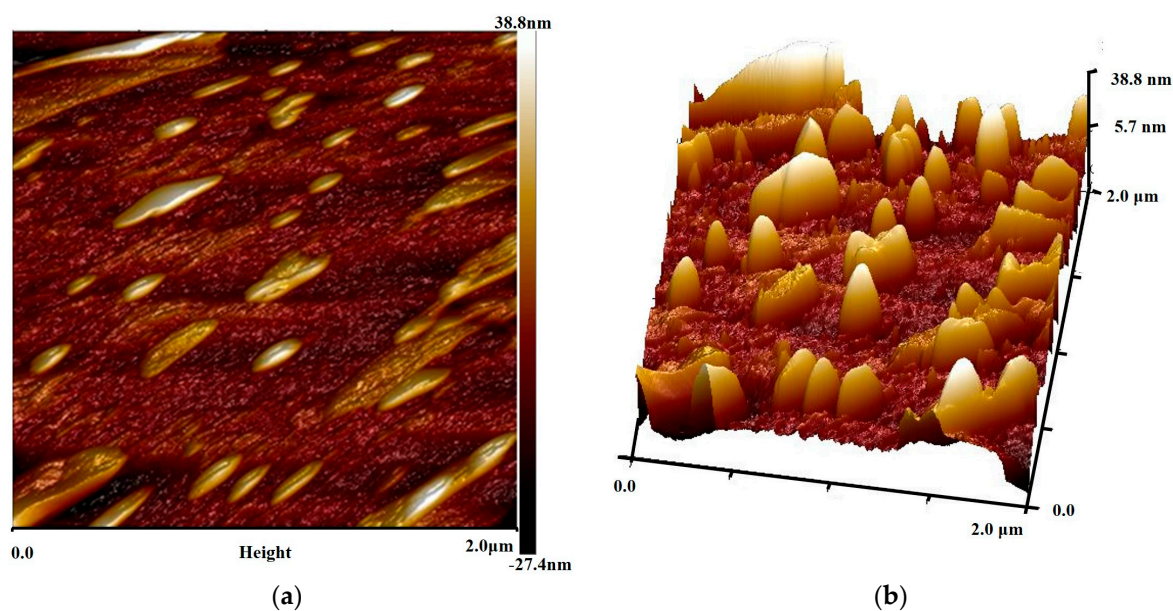

Figure 6. AFM (**a**) 2D and (**b**) 3D images of bacterial adsorption at 0.5 h.

Acidithiobacillus ferrooxidans is a bacillus of 0.2–0.5 μm width and 1.0–2.0 μm length. Figure 7a,b show that the 2D and 3D images of the bacterial adsorption after 8 h differ significantly from Figure 6. Figure 7a shows that the pyrite surface height changed from −198.7 nm to 256.8 nm, which is consistent with the bacterial size. Some elliptical pits were present on the pyrite surface (marked with circle). These could be caused by abscission or death of the adsorbed bacteria. As shown in Figure 7b, bacteria were present on the pyrite and some small colonies had formed, which is consistent with the results in Figure 4. However, the bacteria were independent and did not form a distinct EPS layer.
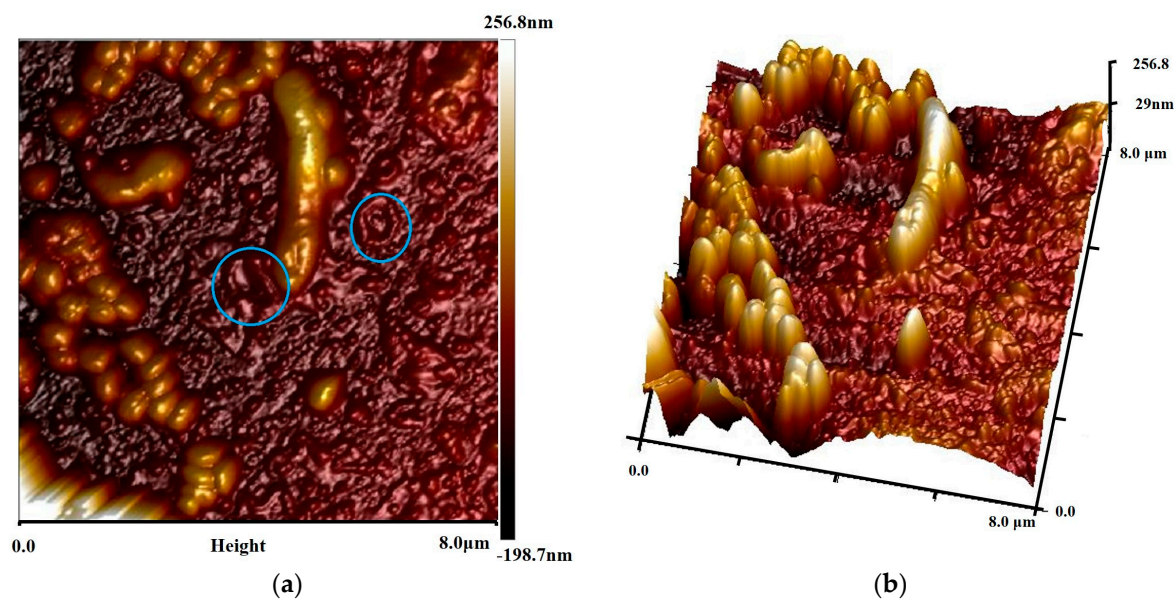
Figure 7. AFM (**a**) 2D and (**b**) 3D images of bacterial adsorption at 8 h.

Figure 8a,b show the 2D and 3D images of bacterial adsorption after 16 h. Compared with Figure 7, the adsorbed bacteria formed colonies on the pyrite surface. The EPS of the bacteria covered each other and formed an EPS layer.
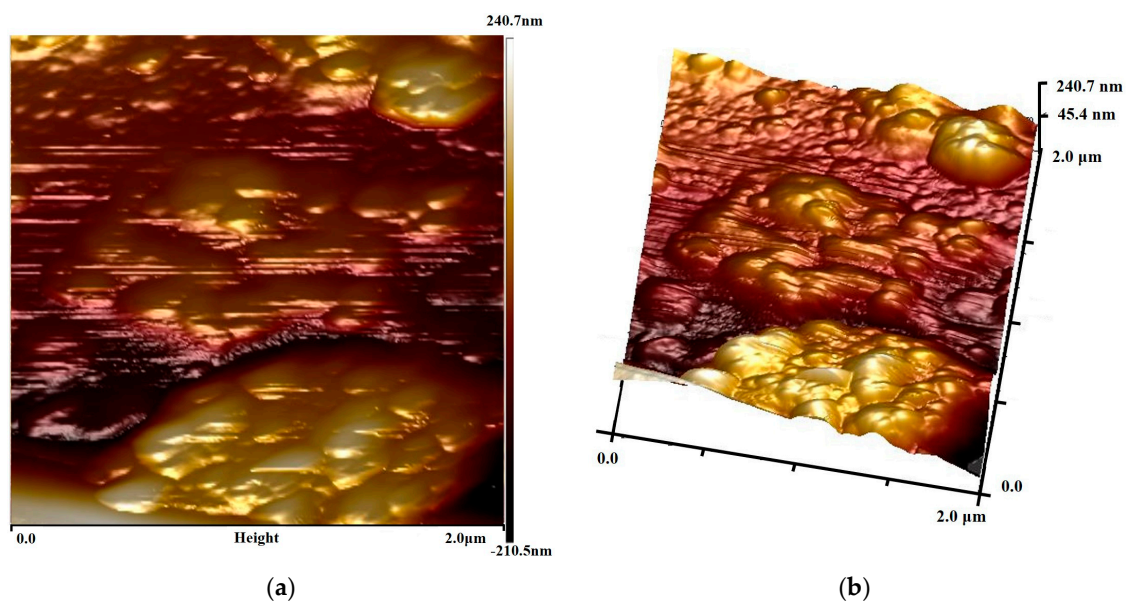

Figure 8. AFM (**a**) 2D and (**b**) 3D images of bacterial adsorption at 16 h.

The experimental results in Sections 3.2 and 3.5 indicated that bacteria could destroy the humic-acid layer on pyrite and the corresponding mechanism as shown in Figure 9. Bacteria can change the EPS secretions on the pyrite surface after contact with the humic-acid layer. The changed bacteria are adsorbed on the surface of the humic-acid layer, and they grow and propagate. Humic-acid stimulates bacteria to secrete more EPS. The secreted EPS layer gradually engulfs the humic-acid layer on the pyrite surface, which enables contact between the bacteria and the pyrite, and increases the pyrite oxidation. The death or shedding of bacteria can remove the phagocytic or adsorb humic-acid, which exposes the pyrite surface and enables contact with the bacteria or Fe^{3+} to promote the oxidation of pyrite.
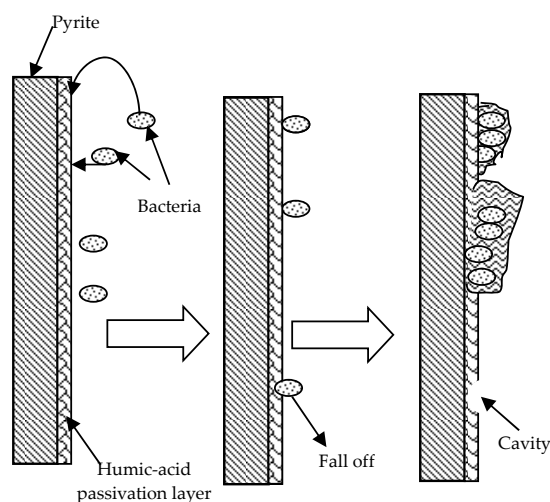
Figure 9. Mechanism of destruction of humic-acid passivation layer by bacteria.

4. Conclusions

AFM showed that the humic-acid adsorbed on the pyrite surface and formed a passivation layer. Bacteria could adsorb on the surface of the pyrite with the humic-acid layer. Although the humic-acid layer slowed the speed of bacterial adsorption onto the pyrite surface, it did not change the number of bacteria adsorbed on the pyrite. The bacteria that adsorbed on the pyrite surface reproduced to form colonies, and the EPS could interconnect.

The bacteria could adsorb or phagocytose humic-acid by EPS and destroy the humic-acid passivation layer. Therefore, bacteria and Fe^{3+} in solution could contact the pyrite directly and improve the pyrite oxidation significantly.

References

1. Large, R.R.; Bull, S.W.; Valeriy Maslennikov, V.V. A Carbonaceous Sedinetary Source-Rock Model for Carlin-Type and Orogenic Gold Deposits. *Econ. Geol.* **2011**, *106*, 331–358. [CrossRef]
2. Cook, N.J.; Chryssoulis, S.L. Concentrations of invisible gold in the common sulfides. *Can. Miner.* **1990**, *28*, 1–16.
3. Pyke, B.L.; Johnston, R.F.; Brooks, P. The characterization and behavior of carbonaceous material in a refractory gold bearing ore. *Miner. Eng.* **1999**, *12*, 851–862. [CrossRef]
4. Radtke, A.S.; Scheiner, B.J. Studies of hydrothermal gold deposition (I), carlin gold deposit Nevada: The role of carbonaceous materials in gold deposition. *Econ. Geol.* **1976**, *65*, 87–102. [CrossRef]
5. Nelson, J.H.; Macdougall, J.J.; Baglin, F.G.; Freeman, D.W.; Nadler, M.; Hendrix, J.L. Characterization of Carlin-Type Gold Ore by Photoacoustic, Raman, and EPR Spectroscopy. *Appl. Spectrosc.* **1982**, *36*, 574–576. [CrossRef]
6. Temminghoff, E.J.M.; Van der Zee, S.E.A.T.M.; de Haan, F.A.M. Copper mobility in a copper-contaminated sandy soil as affected by pH and solid and dissolved organic matter. *Environ. Sci. Technol.* **1997**, *31*, 1109–1115. [CrossRef]

7. Murphy, E.M.; Zzchara, J.M. The role of sorbed humic substances on the distribution of organic and inorganic contaminants in groundwater. *Geoderma* **1995**, *67*, 103–124. [CrossRef]
8. Bennett, J.W.; Ritchie, A.I.M. A proposed technique for measuring in situ the oxidation rate in bio-oxidation and bio-leach heaps. *Hydrometallurgy* **2004**, *72*, 51–57. [CrossRef]
9. Brierley, J.A. Response of microbial systems to thermal stress in biooxidation-heap pretreatment of refractory gold ores. *Hydrometallurgy* **2003**, *71*, 13–19. [CrossRef]
10. Pradhan, N.; Nathsarma, K.C.; Rao, S.K.; Sukla, L.B.; Mishra, B.K. Heap bioleaching of chalcopyrite: A review. *Miner. Eng.* **2008**, *21*, 355–365. [CrossRef]
11. Cruz, F.L.S.; Oliveira, V.A.; Guimarães, D.; Souza, A.D.; Leão, V.A. High-temperature bioleaching of nickel sulfides: Thermodynamic and kinetic implications. *Hydrometallurgy* **2010**, *105*, 103–109. [CrossRef]
12. Liu, Y.G.; Zhou, M.; Zeng, G.M.; Wang, X.; Fan, T.; Xu, W.H. Bioleaching of heavy metals from mine tailings by indigenous sulfur-oxidizing bacteria: Effects of substrate concentration. *Bioresour. Technol.* **2008**, *99*, 4124–4129. [CrossRef] [PubMed]
13. Belzile, N.; Maki, S.; Chen, Y.W.; Goldsack, D. Inhibition of pyrite oxidation by surface treatment. *Sci. Total. Environ.* **1997**, *196*, 177–186. [CrossRef]
14. Acai, P.; Sorrenti, E.; Gornerb, T.; Polakovic, M.; Kongolo, M.; de Donato, P. Pyrite passivation by humic-acid investigated by inverse liquid chromatography. *Colloid Surf. A Physicochem. Eng.* **2009**, *337*, 39–46. [CrossRef]
15. Lalvani, S.B.; DeNeve, B.A.; Weston, A. Prevention of Pyrite Dissolution in Acidic Media. *Corrosion* **1991**, *47*, 55–61. [CrossRef]
16. Fein, J.B.; Boily, J.; GüÇlü, K.; Kaulbach, E. Experimental study of humic-acid adsorption onto bacteria and Al-oxide mineral surfaces. *Chem. Geol.* **1999**, *162*, 33–45. [CrossRef]
17. Zhou, J.; Niu, Y.; Qiu, G.; Qin, W. Protein content of mineral-adhered bacterium by ninhydrin colorimetric method. *J. Cent. South Univ. Technol.* **2003**, *34*, 128–131.
18. Xing, Y.; Gui, X.; Pan, L.; Pinchasik, B.E.; Cao, Y.; Liu, J.; Kappl, M.; Butt, H.J. Recent experimental advances for understanding bubble-particle attachment in flotation. *Adv. Colloid Interface Sci.* **2017**, *246*, 105–132. [CrossRef] [PubMed]
19. Xing, Y.; Xu, M.; Gui, X.; Cao, Y.; Babel, B.; Rudolph, M.; Weber, S.; Kappl, M.; Butt, H.J. The application of atomic force microscopy in mineral flotation. *Adv. Colloid Interface Sci.* **2018**, *256*, 373–392. [CrossRef] [PubMed]
20. Frølund, B.; Palmgren, R.; Keiding, K.; Nielsen, P.H. Extraction of extracellular polymers from activated sludge using a cation exchange resin. *Water Res.* **1996**, *30*, 1749–1758. [CrossRef]
21. Vakondios, N.; Koukouraki, E.E.; Diamadopoulos, E. Effluent organic matter (EfOM) characterization by simultaneous measurement of proteins and humic matter. *Water Res.* **2014**, *63*, 62–70. [CrossRef] [PubMed]
22. Poglazova, M.; Mitskevich, I.; Kuzhinovsky, V. A spectrofluorimetric method for the determination of total bacterial counts in environmental samples. *J. Microbiol. Meth.* **1996**, *24*, 211–218. [CrossRef]
23. Blake, R.C.; Shute, E.A.; Howard, G.T. Solubilization of minerals by bacteria: Electrophoretic mobility of Thiobacillus ferrooxidans in the presence of iron, pyrite, and sulfur. *Appl. Environ. Microbiol.* **1994**, *60*, 3349–3357. [PubMed]
24. Sand, W.; Gehrke, T.; Jozsa, P.; Schippers, A. (Bio)chemistry of bacterial leaching—Direct vs. indirect bioleaching. *Hydrometallurgy* **2001**, *59*, 159–175. [CrossRef]
25. Yu, R.; Ou, Y.; Tan, J.; Wu, F.; Sun, J.; Zhong, D. Effect of EPS on adhesion of Acidithiobacillus ferrooxidans on chalcopyrite and pyrite mineral surfaces. *Trans. Nonferrous Met. Soc. China* **2011**, *21*, 407–412. [CrossRef]
26. Gehrke, T.; Telegdi, J.; Thierry, D.; Sand, W. Importance of Extracellular Polymeric Substances from Thiobacillus ferrooxidans for Bioleaching. *Appl. Environ. Microbiol.* **1998**, *64*, 2743–2747. [PubMed]
27. Lehman, M.R.; O'Connell, S.P. Comparison of extracellular enzyme activities and community composition of attached and free-living bacteria in porous medium columns. *Appl. Environ. Microbiol.* **2002**, *68*, 1569–1575. [CrossRef] [PubMed]